Results in Physics 12 (2019) 1809–1813

Contents lists available at ScienceDirect

Results in Physics

journal homepage: www.elsevier.com/locate/rinp

Low temperature thermoluminescence of Gd_2O_3 nanoparticles using various heating rate and $T_{max} - T_{exc.}$ methods

Serdar Delice[a,*], Mehmet Isik[b], Nizami M. Gasanly[c,d]

[a] Department of Physics, Hitit University, 19040 Çorum, Turkey
[b] Department of Electrical and Electronics Engineering, Atilim University, 06836 Ankara, Turkey
[c] Department of Physics, Middle East Technical University, 06800 Ankara, Turkey
[d] Virtual International Scientific Research Centre, Baku State University, 1148 Baku, Azerbaijan

ARTICLE INFO

Keywords:
Lanthanide oxides
Gd_2O_3
Thermoluminescence
Defects

ABSTRACT

Thermoluminescence (TL) measurements for Gd_2O_3 nanoparticles were carried out for various heating rates between 0.3 and 0.8 K/s at low temperatures (10–280 K). TL spectrum exhibited two observable and one faint peaks in the temperature region of 10–100 K, and four peaks in the temperature region of 160–280 K. Heating rate analysis was achieved to understand the behaviors of trap levels. It was seen that the peak maximum temperatures and TL intensities of all peaks increase with increasing heating rate. This behavior was ascribed to anomalous heating rate effect. $T_{max} - T_{exc.}$ analysis was accomplished for TL peaks at relatively higher temperature region to reveal the related traps depths. $T_{max} - T_{exc.}$ plot presented a staircase structure indicating that the TL glow curve is composed of well separated glow peaks. Mean activation energies of trapping centers corresponding to these separated peaks were found as 0.43, 0.50, 0.58 and 0.80 eV.

Introduction

Rare earth oxide nanoparticles have been widely studied by researchers owing to their unique physical and chemical properties. These promising nanomaterials have been fascinated enormous interest for investigation of their possible usability in different fields of device applications. They may take roles in part of devices such as optoelectronics, sensors, detectors, catalysts, luminescent and biomedical devices [1–5]. Gd_2O_3 is one of the rare earth oxide materials and has significant and particular properties. High value of spin magnetic moment $s = 7/2$ makes this material applicable for magnetic resonance imaging [6,7]. Also, Gd_2O_3 is capable of absorbing x-ray at a high rate so that it can be convenient to applications like x-ray computed biomedical devices [8,9]. This material possesses good thermal stability, low phonon energy, large optical band gap (5.4 eV) and lower lasing threshold [10]. In respect of these properties, Gd_2O_3 is an encouraging host material which can be easily doped with rare earth ions having high luminescence efficiency [11]. The most efficient and useful dopants are Eu^{3+}, Er^{3+} and Yb^{3+} ions. It has been found that Gd_2O_3 has high luminescence efficiency and can be used in various applications as it is doped with Er^{3+} and Yb^{3+} ions [12]. The doped Gd_2O_3 with these ions possesses very high multicolor upconversion emission [13]. Eu doped Gd_2O_3 is also perfect red-emission material which can be used for display and lamp applications [14].

Previously, photoluminescence (PL) and thermoluminescence (TL) investigations were achieved and reported for Gd_2O_3 phosphor [15]. The PL measurements were performed in the wavelength range of 400–700 nm. Two emission bands centered at 490 and 545 nm were observed in PL spectrum. TL experiments were carried out above room temperature after 1 kGy γ-rays exposure of undoped Gd_2O_3. One broad TL glow peak with maximum temperature of 226.4 °C was observed in the TL spectrum. Activation energy related to this peak was reported as 0.6759 eV. Eu^{3+} doped Gd_2O_3 nanoparticles were studied in terms of cathodoluminescence and PL measurements for different dopant rates [16]. Both of the measurements showed that Gd_2O_3:Eu^{3+} has red emission at 612 nm. Yb^{3+} doped Gd_2O_3 phosphor was studied by virtue of PL experiments performed in the wavelength range of 350–1100 nm [17]. Five PL emission peaks centered at 364, 489, 545,590 and 624 nm in visible region and three emission peaks at 965, 1020 and 1064 nm in near infrared region were revealed from the measurements. The variation of luminescence emission was investigated for different Yb^{3+} ion concentration. PL measurements of Gd_2O_3:Dy^{3+} phosphor was also accomplished above room temperature in the wavelength region of 450–700 nm [18]. Three PL emission peaks were observed at 486, 572 and 669 nm.

Heating rate is a significant parameter influencing the stimulation of charge carriers occupying trap centers in materials. Throughout TL

* Corresponding author.
E-mail address: serdardelice@hitit.edu.tr (S. Delice).

https://doi.org/10.1016/j.rinp.2019.02.025
Received 17 January 2019; Received in revised form 7 February 2019; Accepted 7 February 2019
Available online 11 February 2019

investigations, the effect of variable heating rate has been studied by many researchers to comprehend the behavior of TL peaks. It is well-known that increasing heating rate leads TL peak to shift towards higher temperatures and TL intensity to decrease on condition that integral area of TL peak remains constant. However it was also shown that both TL intensity and peak area decreased and increased in different variable heating rate studies. These phenomena have been called as thermal quenching and anomalous heating rate, respectively. In the present study, low temperature (10–280 K) TL investigations of Gd_2O_3 nanoparticles have been achieved with various heating rates between 0.3 and 0.8 K/s. Heating rate behaviors of observed TL peaks have been explored by analyzing the TL spectra. Variable heating rate behavior of experimentally obtained TL peaks have been ascribed to anomalous heating rate effect. Traps depths have also been investigated using $T_{max} - T_{exc.}$ plot. Single trap levels have been attributed for the related TL peaks by utilizing this plot. Activation energies of these traps have been obtained.

Experimental

Gd_2O_3 nanoparticles used for TL investigations were supplied from Alfa Aesar. Thermoluminescence measurements were applied on three aliquots of pellet forms of the nanopowders. The pellets of ~0.58 g were in the shape of disks with diameter of 10 mm and thickness of ~1 mm. Thermoluminescence measurements were carried out with a setup built around a closed cycle helium gas cryostat (Advanced Research Systems, Model CSW 202) that can keep the environment at low temperatures (10–300 K). The Gd_2O_3 sample was placed to the cryostat by a thermally conductive holder. Lakeshore Model 331 temperature controller which can ramp the temperature linearly at a maximum rate of 1.2 K/s was employed to keep the temperature of the sample at an intended value. For TL measurements performed with various heating rates, the temperature was decreased to $T_0 = 10$ K and the sample was exposed to UV light (~220 nm) (Ocean Optics; D-2000 Deuterium Light Source). After the illuminator was switched off, 5 min was waited to bring the charge carriers to equilibrium. Then, the sample was heated up to 280 K with different heating rates between 0.3 and 0.8 K/s. For the TL experiments with different excitation temperatures ($T_{exc.}$ = 80–170 K), the temperature was adjusted to an intended $T_{exc.}$ and the sample was exposed to the UV light. Then, the temperature was decreased to T_0 and the sample was heated up to 280 K with a constant heating rate of 0.3 K/s. The emitted luminescence was focused to photomultiplier (PM) tube (Hamamatsu R928, spectral response: 185–900 nm) by a lens which attached to the optical access port of the cryostat with quartz window. The pulses that were generated by PM tube were converted into TTL pulses (0–5 V) via a fast amplifier/discriminator (Hamamatsu Photon Counting Unit C3866). TTL pulses were counted by the counter of a data acquisition module (National Instruments, NI 6211). All of the measurement setup were managed with a central system by improving a software written in LabView (National Instruments).

Results and discussion

Anomalous heating rate behavior of TL glow peaks

Throughout the TL investigations achieved for various heating rates, different heating rate behaviors of trap levels have been experienced in studied semiconductors and insulators due to the different characteristics of trapped charge carriers. Normally, according to TL theory the expected event is that the TL intensity of glow curves decreases and the integrated area remains constant as elevating heating rates are employed sequentially. However, for many luminescent materials both TL intensity and area enclosed under the glow curves were found to decrease with increasing heating rates. This event was explained with the phenomenon called as thermal quenching [19]. In recent years, opposite behavior which the TL intensity increases with increasing heating rates has been reported in the study on YPO_4 crystals [20]. The observed behavior was explained with the models called as two-stage TL [21] and semi-localized transition (SLT) [22,23] models. Two-stage TL model takes into consideration the presence of a localized excited state from which the electrons are released into the conduction band. Radiative recombination of electrons through only the conduction band is taken into account in this model. The SLT model considers also the direct non-radiative transitions of electrons from excited states into recombination center besides the radiative recombination taken place in two-stage TL model. At lower heating rates the probability of non-radiative transitions is higher since trapped electrons stay longer at excited state that causes decreasing the probability of stimulation of electrons into the conduction band. At higher heating rates the stimulation probability increases thanks to decrease in occupancy time at excited states. This leads to increase of emitted luminescence providing TL peaks to have higher intensity. This behavior is called as anomalous heating rate effect that has recently been observed and reported for Ce^{3+} doped ZnB_2O_4 phosphor [24], household salt [25], GaS [26] and Tl_2GaInS_4 [27] single crystals, Sm^{3+} and Tb^{3+} doped $BaAl_2O_4$ phosphors [28] and La-doped zinc borate [29]. Such a behavior has also been observed in the present TL study on Gd_2O_3 accomplished at low temperatures (10–280 K) for various heating rates between 0.3 and 0.8 K/s as seen in Fig. 1a and b. Although seven peaks labeled as A, B, C, D, E, F and G are available in the TL spectrum, we analyzed the peaks except B and G which did not present certain and comparable peak positions and intensities for analyses. Backgrounds were subtracted from the TL curves before analyses were achieved. As shown in Fig. 1a and b, the peak maximum temperatures (T_{max}) of the peaks shift towards higher temperatures. This behavior was explained by Anishia et al. [30]. Excitation of trapped charge carriers with a lower rate β_1 causes the carriers to occupy trapping levels much more time at temperature T_1. The occupancy of these levels by charge carriers liberated with β_2 will take less at that temperature. As a result, concentration of charge carriers stimulated into conduction band with β_2 at T_1 diminishes as compared with β_1. A temperature T_2 ($T_2 > T_1$) is required for releasing of same amount of charge carriers with β_2. Therefore, the T_{max} of the TL curve increases with elevating heating rate. As seen from the figures, TL intensities of glow peaks increase with raising rates. The integrated areas also exhibit increasing tendency. The areas enclosed under the TL peaks A and C enhance approximately 125 and 220 percent as the heating rate is increased from 0.3 to 0.8 K/s. The total integrated area of the TL curve consisting of peaks D, E and F raises about 230 percent. These enhancements were attributed to anomalous heating rate effect. Fig. 2 depicts the heating rate variations of TL intensities and T_{max} values of the peaks A, C, D, E and F. As seen from the figure, the TL intensities increase with increasing heating rate. Moreover, peak maximum temperatures shift from 32 to 46 K, 62 to 86 K, 172 to 224 K, 194 to 244 K, and 226 to 276 K for peaks A, C, D, E and F, respectively.

Determination of traps depths

There are two empirical methods to separate overlapping TL peaks appearing due to closeness of a series of single trap levels or due to continuously distributed trap levels. The well-known one is based on

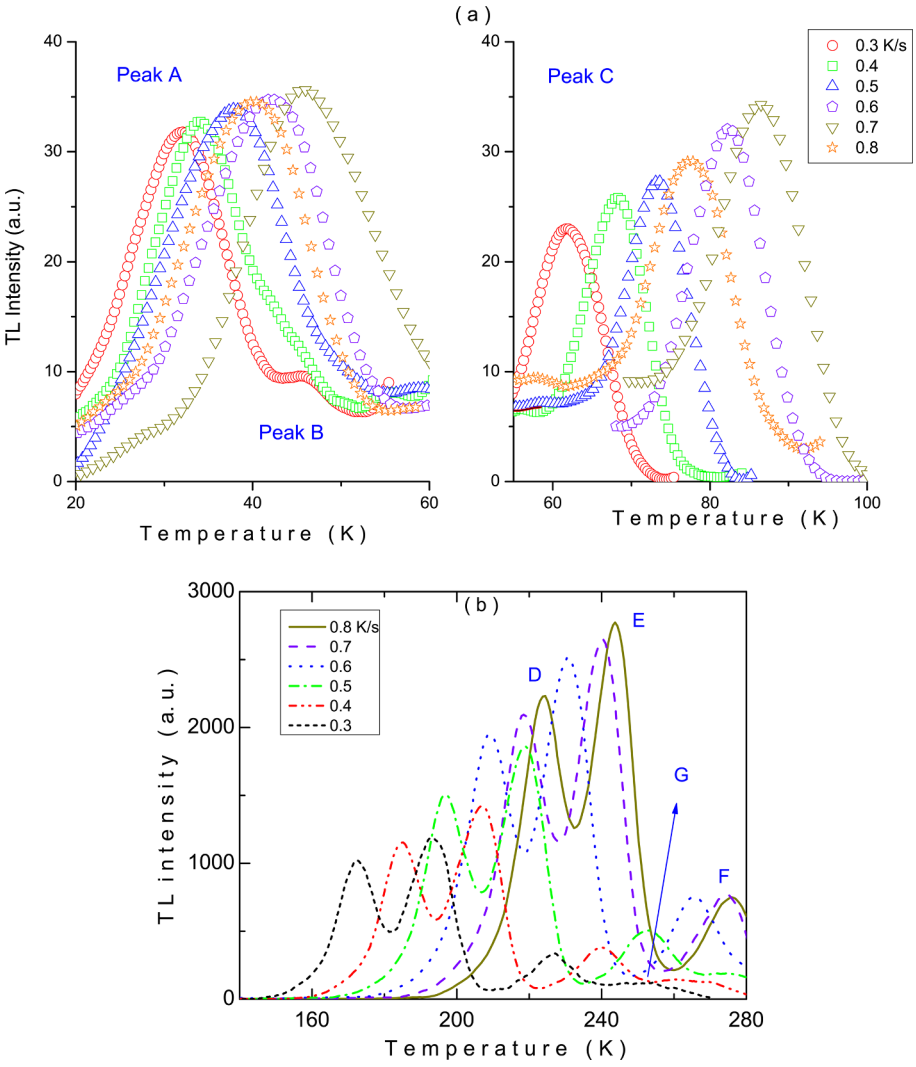

Fig. 1. Experimental TL peaks of Gd_2O_3 nanoparticles detected with various heating rates between 0.3 and 0.8 K/s (a) for peaks A and C in the temperature region of 10–100 K (b) for peaks D, E and F in the temperature region of 160–280 K.

pre-heating treatment up to stopping temperature (T_{stop}) before detecting a TL curve [31]. Alternatively, the second method which is based on the excitation of sample at different temperature ($T_{exc.}$) and recording TL curve between starting and end temperatures was used by some researchers [32,33]. Fundamentally, both of the methods can be used to empty the shallowest trap levels up to T_{stop} ($T_{exc.}$) and so to obtain TL peaks arising from remaining levels. In order to elucidate the nature and characteristics of trapping levels associated with observed TL peaks of Gd_2O_3 nanoparticles, we applied latter technique to the observed TL curve at $T_0 = 10$ K. The implementation of this technique was achieved as the following: The temperature of the environment was brought to an excitation temperature and the sample was exposed to the UV light at this temperature. After stopping the radiation source, the sample was cooled to initial temperature of $T_0 = 10$ K. Then, the temperature of the sample was increased from $T_0 = 10$ to 300 K and emitted luminescence intensity was recorded as a function of temperature. The successive experiments were accomplished for different $T_{exc.}$ values ranging from 80 to 170 K with constant heating rate of 0.3 K/s. By this way, shallowest trapping levels were completely or partially cleaned from charge carriers and only the remaining levels contributed to emitted luminescence, resulting in gradually disappearing of the TL peaks at lower temperature regions. This method was only applied to TL curve consisting of TL peaks D, E, F and G since the TL intensities of the peaks arising at lower temperature region (peaks A, B and C) were too low to measure and analyze. Fig. 3 illustrates the TL glow curves detected for above mentioned $T_{exc.}$ values. As understood from the figure, the TL intensity and integrated total area of the curves decreased with increasing $T_{exc.}$ due to the decrease of trapped charge carrier concentration. The peak D existed for the $T_{exc.}$ values of 80–120 K and disappeared as the $T_{exc.}$ = 130 K were employed. The peak E was available for $T_{exc.}$ values between 80 and 140 K and depleted at $T_{exc.}$ = 150 K. After 150 K, the peaks F and G were observed up to $T_{exc.}$ = 170 K.

McKeever reported different behaviors of T_{max} dependency on stopping temperature [31]. According to researcher, there are two behaviors for overlapped peaks. $T_{max} - T_{stop}(T_{exc.})$ plot presents either "*staircase*" structure or "*continuous line*" of slope ~ 1.0 (see inset of Fig. 4). *Staircase* structure indicates the presence of a series of well separated glow peaks whereas *continuous line* shows the existence of quasi-continuous distribution of peaks. Fig. 4 shows the $T_{max} - T_{exc.}$ plot in which T_{max} corresponds to location of the first local maximum. As seen from the figure, a *staircase* structure appears for observed TL peaks. This means that these peaks are related with well separated glow peaks associated with different single defect centers. Each consecutive TL curve was analyzed using curve fitting method which is very applicable for determination of activation energy (E_t) of trap levels (see Fig. 5) [19]. Activation energies of trapping levels were found to be between 0.48 and 0.52 eV ($E_{tD,mean}$ = 0.50 eV) for peak D, 0.55–0.61 eV

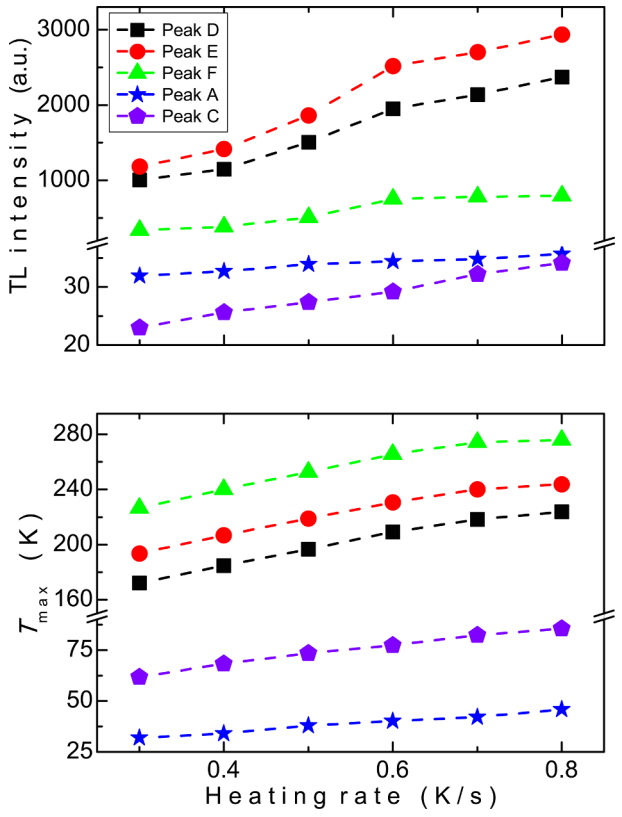

Fig. 2. Heating rate variations of TL intensities and peak maximum temperatures of TL peaks (peaks A, C, D, E and F) obtained for Gd_2O_3 nanoparticles. Dashed lines are only guides for the eye.

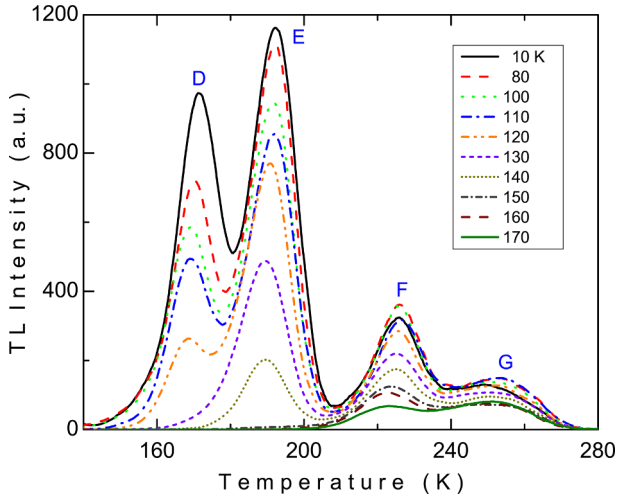

Fig. 3. Experimental TL peaks (peaks D, E, F and G) of Gd_2O_3 nanoparticles recorded for different excitation temperatures between 80 and 170 K.

($E_{tE,mean}$ = 0.58 eV) for peak E, 0.77–0.82 eV ($E_{tF,mean}$ = 0.80 eV) for peak F and 0.42–0.45 eV ($E_{tG,mean}$ = 0.43 eV) for peak G. The frequency factors related to the revealed trap levels were also calculated using the T_{max} and E_t values obtained from curve fitting method [19]. The mean values for frequency factors were found to be 2.6×10^{13}, 9.2×10^{13}, 2.3×10^{14} and 4.9×10^{6} s^{-1} for peaks D, E, F and G, respectively. Here, it is seen that the activation energy of the highest peak (peak G) is smaller than those of other peaks. Generally, as the peak maximum temperature shifts to higher values, the activation energy increases. However, in some cases the situation can be different. The shape and position of the TL peaks depend strongly on the activation energy,

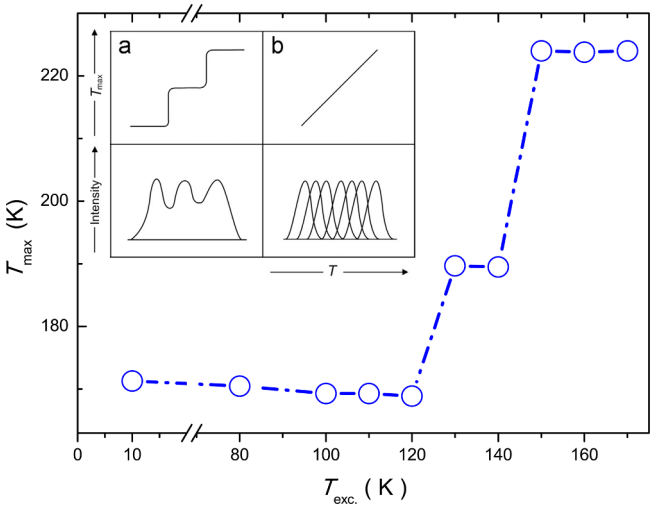

Fig. 4. The $T_{max} - T_{exc.}$ plot for Gd_2O_3 nanoparticles. Inset: TL glow curves and corresponding $T_{max} - T_{exc.}$ plots as proposed by McKeever [31]. (a) series of well separated glow peaks creates a "*staircase*" (b) quasi-continuous distribution of glow peaks presents a *straight line*.

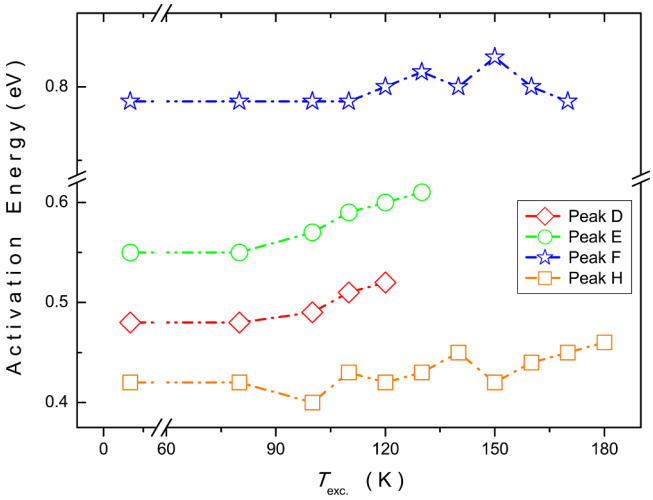

Fig. 5. E_t vs $T_{exc.}$ plots for peaks D, E, F and G. Dashed lines are only guides for the eye.

frequency factor and heating rate. By taking into account the constant heating rate during thermal cleaning procedure, the highest peak with lower activation energy can be observed due to the low frequency factor. There are some examples to this event reported in literature [34–36].

Conclusions

TL studies on Gd_2O_3 nanoparticles were accomplished by analyzing the TL spectra recorded for various heating rates and excitation temperatures between 0.3 and 0.8 K/s and between 80 and 170 K, respectively. The peak maximum temperatures and the TL intensities of the TL peaks were found to shift towards higher temperatures and to increase in magnitude, respectively, with increasing heating rate. Such a behavior was attributed to phenomenon called as anomalous heating rate effect. The traps depths were also predicted by utilizing an experimental technique. $T_{max} - T_{exc.}$ analysis resulted with the existence of four trap regions having mean activation energies of 0.43, 0.50, 0.58 and 0.80 eV. The lower activation energy of the peak having highest peak maximum temperature was thought to be caused due to the

retrapping of charge carriers into the shallower trap levels and/or due to low frequency factor.

References

[1] Kenyon AJ. Recent developments in rare-earth doped materials for optoelectronics. Prog Quantum Electron 2002;26:225–84.
[2] Tokoro H, Fujii S, Oku T. Microstructures and magnetic properties of boron nitride- and carbon-coated iron nanoparticles synthesized by a solid phase reaction. J Mater Chem 2004;14(2):253–7.
[3] Nichkova M, Dosev D, Gee SJ, Hammock BD, Kennedy IM. Microarray immunoassay for phenoxybenzoic acid using polymer encapsulated Eu:Gd2O3 nanoparticles as fluorescent labels. Anal Chem 2005;77:6864–73.
[4] Huang CC, Su CH, Li WM, Liu TY, Chen JH, Yeh CS. Bifunctional Gd2O3/C nanoshells for MR imaging and NIR therapeutic applications. Adv Funct Mater 2009;19:249–58.
[5] Yang P, Gai S, Liu Y, Wang W, Li C, Lin J. Uniform hollow Lu2O3: Ln (Ln = Eu3+, Tb3+) spheres: facile synthesis and luminescent properties. Inorg Chem 2011;50:2182–90.
[6] Lauffer RB. Paramagnetic metal complexes as water proton relaxation agents for NMR imaging: theory and design. Chem Rev 1987;87:901–27.
[7] Caravan P, Ellison JJ, McMurry TJ, Lauffer RB. Gadolinium (III) chelates as MRI contrast agents: structure, dynamics, and applications. Chem Rev 1999;99:2293–352.
[8] Lee EJ, Heo WC, Park JW, Chang Y, Bae JE, Chae KS, Kim TJ, Park JA, Lee GH. D-glucuronic acid coated Gd(IO3)3·2H2O nanomaterial as a potential T1 MRI-CT dual contrast agent. Eur J Inorg Chem 2013;2013:2858–66.
[9] Cheung ENM, Alvares RDA, Oakden W, Chaudhary R, Hill ML, Pichaandi J, Mo GCH, Yip C, MacDonald PM, Stanisz GJ, Van Veggel FCJM, Prosser RS. Polymer-stabilized lanthanide fluoride nanoparticle aggregates as contrast agents for magnetic resonance imaging and computed tomography. Chem Mater 2010;22:4728–39.
[10] Xu L, Yu Y, Li X, Somesfalean G, Zhang Y, Gao H, Zhang Z. Synthesis and upconversion properties of monoclinic Gd2O3:Er3+ nanocrystals. Opt Mater 2008;30:1284–8.
[11] Dosev D, Kennedy IM, Godlewski M, Gryczynski I, Tomsia K, Goldys EM. Fluorescence upconversion in Sm-doped Gd2O3. Appl Phys Lett 2006;88:011906.
[12] Joshi C, Rai A, Dwivedi Y, Rai SB. Color tunable emission from (GdxY1–x) 2O3:Er3+, Yb3+ phosphor prepared by combustion method. J Lumin 2012;132:806–15.
[13] Guo H, Dong N, Yin M, Zhang W, Lou L, Xia S. Visible upconversion in rare earth ion-doped Gd2O3. J Phys Chem B 2004;108:19205–9.
[14] Roh HS, Kang YC, Park SB. Morphology and luminescence of (GdY)2O3: Eu particles prepared by colloidal seed-assisted spray pyrolysis. J Colloid Interface Sci 2000;228:195–9.
[15] Tamrakar RK, Bisen DP, Brahme N. Characterization and luminescence properties of Gd2O3 phosphor. Res Chem Intermed 2014;40:1771–9.
[16] Lin CC, Lin KM, Li YY. Sol–gel synthesis and photoluminescent characteristics of Eu3+-doped Gd2O3 nanophosphors. J Lumin 2007;126:795–9.
[17] Tamrakar RK, Bisen DP, Brahme N. Effect of Yb3+ concentration on photoluminescence properties of cubic Gd2O3 phosphor. Infrared Phys Techn 2015;68:92–7.
[18] Selvalakshmi T, Sellaiyan S, Uedonob A, Bose AC. Investigation of defect related photoluminescence property of multicolour emitting Gd2O3:Dy3+ phosphor. RSC Adv 2014;4:34257–66.
[19] Chen R, McKeever SWS. Theory of thermoluminescence and related phenomena. Singapore: World Scientific; 1997.
[20] Bos AJJ, Poltoon NRJ, Wallinga J, Bessiere A, Dorenbos P. Energy levels in YPO4:Ce3+, Sm3+ studied by thermally and optically stimulated luminescence. Radiat Meas 2010;45:343–6.
[21] Chen R, Lawless JL, Pagonis V. Two-stage thermal stimulation of thermoluminescence. Radiat Meas 2012;47:809–13.
[22] Mandowski A, Bos AJJ. Explanation of anomalous heating rate dependence of thermoluminescence in YPO4:Ce3+, Sm3+ based on the semi-localized transition (SLT) model. Radiat Meas 2011;46:1376–9.
[23] Pagonis V, Blohm L, Brengle M, Mayonado G, Woglam P. Anomalous heating rate effect in thermoluminescence intensity using a simplified semi-localized transition (SLT) model. Radiat Meas 2013;51–52:40–7.
[24] Dogan T, Yuksel M, Akca S, Portakal ZG, Balci-Yegen S, Kucuk N, Topaksu M. Normal and anomalous heating rate effects on thermoluminescence of Ce-doped ZnB2O4. Appl Radiat Isotops 2017;128:256–62.
[25] Yüce UR, Engin B. Effect of particle size on the thermoluminescence dosimetric properties of household salt. Radiat Meas 2017;102:1–9.
[26] Delice S, Bulur E, Gasanly NM. Thermoluminescence in gallium sulfide crystals: an unusual heating rate dependence. Phil Mag 2015;95:998–1006.
[27] Delice S, Bulur E, Gasanly NM. Anomalous heating rate dependence of thermoluminescence in Tl2GaInS4 single crystals. J Mater Sci 2014;49:8294–300.
[28] Kaynar ÜH, Guvener E, Ayvacikli M, Dogan T, Balci-Yegen S, Oglakci M, Topaksu M, Karabulut Y, Canimoglu A, Benourdja S, Can N. Anomalous heating rate response of beta irradiated Sm3+ and Tb3+ doped BaAl2O4 phosphors. J Alloys Compd 2018;764:523–9.
[29] Yüksel M, Dogan T, Balci-Yegen S, Akca S, Portakal ZG, Kucuk N, Topaksu M. Heating rate properties and kinetic parameters of thermoluminescence glow curves of La-doped zinc borate. Radiat Phys Chem 2018;151:149–55.
[30] Anishia SR, Jose MT, Annalakshmi O, Ramasamy V. Thermoluminescence properties of rare earth doped lithium magnesium borate phosphors. J Lumin 2011;131:2492–8.
[31] McKeever SWS. On the analysis of complex thermoluminescence glow-curves: resolution into individual peaks. Phys Stat Sol A 1980;62:331–40.
[32] Van den Eeckhout K, Bos AJJ, Poelman D, Smet PF. Revealing trap depth distributions in persistent phosphors. Phys Rev B 2013;87:045126.
[33] Zeler J, Bolek P, Kulesza D, Zych E. On thermoluminescence mechanism and energy leakage in Lu2O3:Tb, V storage phosphor. Opt Mater X 2019;1:100001.
[34] Kilian A, Bilski P, Gieszczyk W. Thermoluminescence kinetics of undoped and doped (Ti, Cu, Ce) lithium aluminate crystals. Radiat Meas 2017;106:107–12.
[35] Tiwari N, Kuraria RK, Tamrakar RK. Thermoluminescence glow curve for UV induced ZrO2: Ti phosphor with variable concentration of dopant and various heating rate. J Radiat Res Appl Sci 2014;7:542–9.
[36] Isik M, Bulur E, Gasanly NM. Low-temperature thermoluminescence in layered structured Ga0.75In0.25Se single crystals. J Alloys Compd 2012;545:153–6.